# Controlled Drug Release of Modified Mesoporous Silica with Higher Driving Forces Derived from the Accurate Dispersion of Azobenzene Groups

**Yuqing Xue**
China University of Geosciences , Beijing
**Wenqian Zhu**
China University of Geosciences , Beijing
**Wenhui Zhao**
China University of Geosciences , Beijing
**Fengzhu Lv** ( lfz619@126.com )
China University of Geosciences , Beijing
**Sufang Guo**
China University of Geosciences , Beijing
**Yihe Zhang**
China University of Geosciences , Beijing

**Research Article**

**Keywords:** Azobenzene accurate dispersion, mesoporous silica, drug delivery system, UV responsiveness

**Posted Date:** March 9th, 2022

**DOI:** https://doi.org/10.21203/rs.3.rs-1429914/v1

# Abstract

It is highly desirable to design delivery systems that can be activated by stimuli to control the release of guest molecules. So in the present paper two kinds of mesoporous silica (m-$SiO_2$) with amino and azobenzene groups accurately dispersed in different position of the pores were prepared based on the reactivity difference of the raw materials and the feeding sequence. The m-$SiO_2$ with the azobenzene groups at the corner of the particles not only had higher loading ability but also could realize high effective light-control release. ~97% of IBU could be released out from the particles under UV irradiation, almost 10 times as much as the m-$SiO_2$ with the azobenzene groups in the out layer of particles with the same composition. The obvious release difference by the two kinds of particles was analyzed based on the arrangement of the segments in the pores of m-$SiO_2$. The conformation change of stack accumulated azobenzene at the core of the particles produced higher driving force for IBU release and decreased the attraction between -$NH_2$ with drug molecules. The afforded mechanism was confirmed by release drug molecules with different length.


# 1. Introduction

Mesoporous silica (m-$SiO_2$) nanoparticles in the field of drug delivery have attracted much attention because they show the characteristics of uniform particle size distribution, unique porous structure in the nanometer range and versatile functionalization[1–4]. However, the delivery of many toxic drugs requires release at target cells or tissues. It is highly desirable to design delivery systems that can be activated by stimuli to control the release of guest molecules. Therefore, various functionalized m-$SiO_2$ nanoparticles triggered by a single stimulus including redox[5, 6], pH[7, 8], temperature[9, 10], enzymes[11, 12], magnetic field[13, 14] and photo-irradiation[15–17] have been successfully used in the field of drug release.

Azobenzene is one of the most widely utilized chromophores for producing photoresponsive materials. It can be reversibly transformed between the trans and cis isomers upon UV–vis light irradiation, exhibiting precise chemical changes in size and polarity[18, 19]. Therefore azobenzene can be used as photo-responsive component for drug release[20, 21].

Core – shell structured magnetic m-$SiO_2$ nanocomposites covalently grafted with light-responsive azobenzene derivatives in the pores integrated magnetic targeting and stimuli-responsive release property. Irradiation with visible light triggered the release of guest molecules loaded in the mesopores[22]. Silica-coated up converting nanoparticles with the inner m-$SiO_2$ modified by azobenzene molecules were synthesized. The azobenzene molecules made possible the release of the anticancer drug doxorubicin from the pore network of the m-$SiO_2$ outer layer by irradiation with near-infrared (NIR) laser light. The release is regulated by the trans-cis photoisomerization of the azobenzene molecules[23]. Additionally, azobenzene is widely used as on-off for drug release by grafting azobenzene groups on the out surface of m-$SiO_2$ and coupling with β-CD. Under visible light irradiation[4, 21, 24, 25], the trans azobenzene moieties hide in the inner cavity of β-CD and cover the gates of the pores, limiting the release

of the drugs. While as the irradiation is changed to UV, the transformation of trans to cis isomer causes the gates of the pores open and release the drugs.

These study confirmed that azobenzene modified mesoporous silica possessed photoresponsive ability for drug delivery, but the position difference of azobenzene groups resulted in different release mechanism. However the UV-release behavior of m-$SiO_2$ with azobenzene groups dispersed in the corner haven't been studied. Also the position difference of azobenzene groups on the contribution of drug loading and release have not been clarified systematically.

In the present work two kinds of m-$SiO_2$ nanoparticles with -$NH_2$ and azobenzene groups accurately dispersed in the core or out layer of m-$SiO_2$ were prepared via simple one-pot method based on the reactivity difference of the raw materials and the feeding sequence. The core-shell structure was confirmed by TEM, XPS and Z-potential. The release difference of the two kinds of m-$SiO_2$ was compared in detail. The contribution of the position difference of azobenzene groups in the pores of silica on the release were analyzed carefully based on the arrangement and the interaction of m-$SiO_2$ segments with IBU. Also the afforded mechanism was confirmed by releasing drugs with different molecule length. The m-$SiO_2$ with the azobenzene groups in the corner of the particles not only had higher loading ability but also could realize high effective light-control release.

## 2. Experimental Section

# 2.1 Materials.

Tetraethyl orthosilicate (TEOS), (3-aminopropyl)triethoxysilane (APTES), ibuprofen (IBU), olsalazine, aspirin, cetyl trimethylammonium bromide (CTAB) were from Jing wen Chemical Reagent Co., Ltd. (3-isocyan-atopropyl)-triethoxysilane and 4-aminoazobenzene were from Yi xiu bo gu Chemical Reagent Co., Ltd. All other chemicals and reagents were obtained from Chemical Reagent Beijing Co., Ltd. (Beijing, China). These reagents were all analytical grade and used without purification.

# 2.2 Preparation of TSUA.

4-(3-TriethoxySilylpropylUreido)Azobenzene (TSUA) was first synthesized according to documented method[26]. 2.74 g of (3-isocyan-atopropyl)-triethoxysilane was added into 24 ml of THF containing 4-aminoazobenzene (3.16 g). The mixture was heated to 313K under reflux and an atmosphere of $N_2$ for 12 h. The obtained solids were recrystallized in hexane/THF at 0°C for five days. The obtained shiny needle-like crystals were centrifuged and washed with hexane for three times. The solid was dried in vacuum at 353K to give TSUA.

# 2.3 Preparation of azobenzene and amino modified m-$SiO_2$.

For preparation of azobenzene groups dispersed in the out layer of m-silica, 0.5 g of CTAB and 0.14 g of NaOH were dissolved in $H_2O$ (240 mL) and stirred for 1h at 353K to form a stable and uniform mixture. A

solution of TEOS (2.5 ml), TSUA, and APTES in ethanol (20 mL) were then added to the above solution slowly. The ratio of TEOS to the whole weight of APTES and TSUA was 10:3. And the feed ratio of APTES to TSUA was 8:2. The mixture was then stirred at 353K for 8 hours. The obtained yellow solids were recovered by filtration and extensively washed with deionized $H_2O$ and ethanol for three times.

The above as-synthesized yellow particles were heated under reflux in ethanol (100 mL) containing 12M HCl (1mL) at 313 K for 6h. The sediment was collected and washed with ethanol and deionized $H_2O$ for two times respectively, and this process was carried out twice to ensure the complete removal of the surfactant. Finally the collected sediment was dried at 353K to yield azobenzene/amino-modified mesoporous silica and assigned as $SiO_2$-TSUA.

For preparation of azo groups dispersed in the core of m-silica, 0.5 g of CTAB and 0.14 g of NaOH were dissolved in $H_2O$ (240 mL) and stirred for 0.5 h at 353K to form a stable and uniform state. Then ethanol solution of TSUA was dropwised to the above system. After 0.5 h, different proportions of TEOs and APTES were added. The ratio of TEOS to the whole weight of APTES and TSUA was 10:3. And the feed ratio of APTES to TSUA was 8:2. The separation and purification steps were the same as for preparation of $SiO_2$-TUSA. The resulting samples were named as TSUA-$SiO_2$.

# 2.4 Drug loading and controlled-release.

100 mg of synthesized samples were suspended in a IBU/ethanol solution (12 ml, 30 mg/ml) respectively and stirred at room temperature for 3hours. The drug loaded particles were centrifuged, washed with deionized $H_2O$ for several times and dried at 353K.

5mg of IBU-loaded particles was suspended in PBS solution (50 ml) and stirred at room temperature under UV/Vis light irradiation. Then 4ml of the supernatant solution was taken for UV–vis measurement and then returned to the vessel afterward with a 15 min interval. The released amount of IBU as a function of time was then analyzed by UV–vis spectroscopy at 222 nm.

# 2.5 Characterization and measurements.

The Fourier transform infrared (FTIR) spectra in the 4000-400$cm^{-1}$ region were obtained using a Perkin Elmer Spectrum 100 FT-IR spectrometer. KBr was used as a background material and disks of samples/KBr mixtures were prepared to obtain the FT-IR spectra. The morphology of the samples was observed with a scanning electron microscope (SEM, HITACHI S-4800) and transmission electron microscopy (TEM, Tecnai G2 F30) containing mapping system. Before observation the samples were gold spraying for 5 min. UV-vis spectrophotometry (TU1901) was used to test the UV-vis adsorption of the release solution and the peaks at 222 nm were performed to determine the release of IBU according to the standard curves of UV-vis adsorption of IBU via concentrations. The specific surface areas and pore volumes of all samples were measured by the Brunauer-Emmett-Teller (BET) method and Barrett-Joyner-Halenda (BJH) method using nitrogen adsorption and desorption isotherms on a Micromeritics (Autosorb-iQ-2MP, Quanta chrome, USA). Thermal gravimetric analysis (TGA) was performed on Perkin-

Elmer TGA 7 with a heating rate of 10℃/min ranging from 25℃ to 1000℃ in air. X-ray photoelectron spectroscopy (XPS, Thermo escalab 250Xi) was used to investigate the N and C ratio in the samples. Zeta-potential values were measured using Zetasizer NanoZS90.

## 3. Results And Discussion

# 3.1 Synthesis and composition of the particles.

Just as shown in Fig. 1, two kinds of m-$SiO_2$ were synthesized by the simple one pot method based on the feed sequence and reactivity difference of the raw materials. The reactivity order of the raw materials was TEOS > APTES > TUSA. So as TUSA was feed together with the other raw materials, the slow reactivity of TUSA resulted in their location most likely in the out layer of m-$SiO_2$. In order to fabricated particles with azobenzene groups dispersed in the inner layer of the particles, TUSA was added firstly and reacted for a period time and formed network before TEOS and APTES beginning to react. Thus, -$NH_2$ groups in the final particles endowed the samples with higher IBU loading and azobenzene groups caused the sample photo-responsive ability. Also the azobenzene groups located in the core of m-$SiO_2$ produced higher driving force for the IBU release.

FTIR confirmed the composition of the designed nanoparticles. In the spectra of TUSA, $SiO_2$ and $SiO_2$-TSUA shown in Fig. 2a, the broad peaks at 1,100$cm^{-1}$ assigning to the stretching vibrations of Si–O–Si were clearly observed[27]. The peak at 2900$cm^{-1}$ corresponding to the C-H stretching vibration of -$CH_3$ in CTAB disappeared in the spectrum of $SiO_2$-TSUA showing the successful removal of the surfactant[28, 29]. Compared to the spectra of TUSA, the characteristic bands at 1550$cm^{-1}$ and 3060$cm^{-1}$ corresponding to N = N and C-H of azobenzene groups in the spectrum of $SiO_2$-TSUA indicated that the TSUA had grafted onto silica successfully[30]. Meanwhile the broad peak at around 3447$cm^{-1}$ in the spectrum of $SiO_2$ corresponding to stretching vibration of O-H shifted to 3350$cm^{-1}$ in the spectra of $SiO_2$-TSUA indicating that the amino groups were successfully incorporated in silica. The FTIR spectra of TUSA-$SiO_2$ were similar with that of $SiO_2$-TSUA confirming the fact that the samples contained amino and azobenzene groups at the same time.

Zeta potential can directly indicate the surface charge of the particles which reflects the amount of -$NH_2$ groups on the surface of m-$SiO_2$. The Zeta potential of TSUA-$SiO_2$ was higher than the corresponding samples of $SiO_2$-TSUA with the same feed ratio showing higher amount of -$NH_2$ on the surface of TSUA-$SiO_2$ (Fig. 2b). These data strongly confirmed more -$NH_2$ groups dispersed on the out layer of TSUA-$SiO_2$, which meant that the azobenzene groups dispersed in the inner core of TSUA-$SiO_2$ and the reaction performed toward the designed direction.

Thermogravimetric analysis revealed the successful functionalization of m-$SiO_2$ with amino and azobenzene groups. All materials exhibited small weight loss around 100℃ due to the loss of physically

adsorbed water molecules. On the TGA curves of $SiO_2$-TSUA(Fig. 2c) and TUSA-$SiO_2$(Fig. 2d), the weight loss between 250–800°C derived from the decomposition of the organic groups[31] which were about 25.45wt% and 28.99wt% confirming the two samples possessed almost the same amount of organic groups.

# 3.2 Morphology of the nanoparticles.

Morphology observation by SEM showed $SiO_2$-TSUA was a mixture of more irregular rods and less spheres (Fig. 3a), while the morphology of TSUA-$SiO_2$ was almost spheres (Fig. 3b) with average diameter of 99nm (Fig. 3e). TEM observation indicated $SiO_2$-TSUA (Fig. 3c) and TSUA-$SiO_2$ (Fig. 3d) both had radial ordered mesoscopic structure and visual channels. But TSUA-$SiO_2$ showed observable edge between inner dark area and outer light gray area indicating the obvious core-shell structural characteristic.

The location of azobenzene and -$NH_2$ groups was further studied by the energy disperse spectroscopy (EDS). In the spectra of $SiO_2$-TSUA (Fig. 4a) and TSUA-$SiO_2$ (Fig. 4b) the distribution of C and N elements was mapped out. As more azobenzene groups were dispersed in the out layer of m-$SiO_2$, the C sphere of $SiO_2$-TSUA had obvious and clear edge with background. But the C sphere of TSUA-$SiO_2$ had light center and relative dark out layer confirming most azobenzene groups located at the inner of TSUA-$SiO_2$. The N spheres of TSUA-$SiO_2$ and $SiO_2$-TSUA were similar. No obvious N edge was observed due to the difficult detection of N.

Figure 5 was the XPS spectra of $SiO_2$-TSUA and TSUA-$SiO_2$. The peaks located at 284.28, 285.40 and 288.42eV were assigned to C1s in C = C, C = O of azobezene groups, while the peak at 285.5 was C1s with $sp^2$ hybrid orbital derived from azobezene and amino propyl groups[32, 33]. The binding energies of N1s in N = N and $NH_2$ were 401.5 and 399.5eV respectively[32, 34]. The C = O peak integral area of $SiO_2$-TSUA was 3.85% higher than that of TSUA-$SiO_2$ which was 3.63% (Fig. 5c and 5d). The integral area of N1s in N = N was 51.8% obviously higher than $NH_2$(48.62%) (Fig. 5e and 5f). Accordingly, the ratio of azobenzene to -$NH_2$ was calculated to be 1:2.5 which was higher than the feed ratio. These data strongly confirmed that azobenzene groups located in the corner of TSUA-$SiO_2$ and more likely dispersed at the gates of the pores in $SiO_2$-TSUA.

The formation of mesopores in the amino/azobenzene modified m-$SiO_2$ was directly reflected by the nitrogen adsorption-desorption isotherms (Fig. 6a) and corresponding pore size distributions (Fig. 6b). $SiO_2$-TSUA and TSUA-$SiO_2$ exhibit a typical IV isotherm with a H4-type hysteresis loop, indicating the presence of mesopores[35] Stepwise adsorption of nitrogen and capillary condensation at a relative pressure ($P/P_0$) of 0.45 to 0.95 and 0.3 to 0.95 respectively was exhibited. The surface areas, pore diameters and pore volumes of $SiO_2$, $SiO_2$-TSUA and TSUA-$SiO_2$ were 1030 $m^2/g$, 854.426 $m^2/g$, 708.944 $m^2/g$, 3.061 nm, 2.455 nm, 2.453 nm, and 0.493 cc/g, 0.66 cc/g, 0.771 cc/g in order. $SiO_2$-TSUA had

higher surface area, lower pore volume, almost the same pore diameter compared with TSUA-$SiO_2$. The stack accumulation of azobenzene groups in the inner core of TSUA-$SiO_2$ resulted in lower surface area and larger pore volume.

These characterizations confirmed two kinds of m-$SiO_2$ with azobenzene and -$NH_2$ groups accurately dispersed in the inner and out layer were successfully fabricated. The position of azobenzene on m-$SiO_2$ can be controlled just by adjustment the feeding sequence based on the reaction difference of the raw materials.

# 3.3 Photoresponsive ability of the particles

UV-Vis spectroscopic measurements shown in Fig. 7 indicate the successful immobilization of TSUA on the particle surface. Upon UV light irradiation, the absorption band centered at 358 nm declines remarkably, and concurrently the band centered at 450 nm increases a little which ascribed to π-π* transition of the (E)-azobenzene group and n-π* transitions of (Z)-azobenzene group form respectively. The change of the absorption bands induced by UV irradiation indicates the trans-to-cis photoisomerization of the azobenzene. When the nanoparticle was exposed to visible light, the π-π* absorption increases and the n-π* absorption decrease, which implied the process of back-conversion from cis to trans form. All these changes exhibited reversible trans–cis isomerization and photoresponsive ability of TSUA-$SiO_2$[36, 37]. $SiO_2$-TSUA showed the curves similar to TSUA-SiO2.

# 3.4 Loading and release of IBU by the particles

According to the TGA data (Fig. 2b), the loading amount of IBU by $SiO_2$-TSUA and TSUA-$SiO_2$ were 16.12% and 19.0% respectively after comparison the weight loss of particles before and after loading IBU. TSUA-$SiO_2$ had larger loading ability which may derive from the stack accumulation of azobenzene groups in the core and leave more volume in the out part of the pores. The decrease of Zeta potential of the particles after loading of IBU (Fig. 2c) also showed the successful loading of IBU and the larger loading ability of TSUA-$SiO_2$ as the negative charge of IBU neutralized part of the positive charges of the m-$SiO_2$.

The release of IBU from $SiO_2$-TSUA was shown in Fig. 8a. The release amount of IBU from $SiO_2$-TSUA under UV light was higher than that under visible light. Just as shown in Fig. 1, as the loading of IBU was performed under visible light, the azobenzene groups in m-$SiO_2$, which existed as trans form, experienced conformation transformation under UV light irradiation process. This process caused free volume decrease in the pore and driving force formation for IBU release. But the IBU release amount by $SiO_2$-TSUA was very low and less than 55%. While the IBU release percent by TSUA-$SiO_2$ under UV reached up to ~ 93% in 250 min, almost 2 times as much as the m-$SiO_2$ with the azobenzene groups in the out layer of particles with the same composition. Also the release rate difference has increased significantly after 160 min under different release light and rapid release rate under UV light were observed. The reason causing the obvious release behavior difference of the two kinds of particles was shown in Fig. 9. As

azobenzene located in the inner layer of the pores, the organic groups accumulated tightly on the surface of the pores. Under UV radiation, conformation change decreased the free volume in the pores and produced large pushing force which decrease the attraction between -$NH_2$ with the drug molecules. Thus the drug molecules released out rapidly. While as azobenzene was in the out layer of the pores, the organic groups arranged on the surface of the pores loosely as more space was existed especially at the gate of the pores. The volume change of azobenzene groups had no obvious influence on the interaction between -$NH_2$ and drug molecules. So less drug molecules was released out. Therefore the higher IBU release percent by TSUA-$SiO_2$ was due to the conformation change of stack azobenzene groups which produced large pushing forces to the drug molecules.

# 4. Conclusions

Two kinds of m-$SiO_2$ with azobenzene groups accurately dispersed in the core or out layer of m-$SiO_2$ were prepared via a simple one-pot method based on the reactivity difference of the raw materials and the feed sequence. Amino groups endowed the particles enhanced drug loading ability and the azobenzene groups enabled the light driving ability for drug release. The position of azobenzene groups caused the particles show great different release behaviors. The m-$SiO_2$ with the azobenzene groups in the corner of the particles not only had higher IBU loading ability but also could realize high effect light-control release (almost 2 times as much as the m-$SiO_2$ with the azobenzene groups in the out layer of particles with the same feed ratio). ~93% of IBU could be released out under UV irradiation. The higher release of drugs derived from the conformation and occupied space change of the stack accumulated azobenzene groups which resulted in larger pushing force toward the drug molecules.

# Declarations


### Acknowledgement

This work was supported by the Fundamental Research Funds for the national keyi projects (2017YFC0703105).


### Declaration of competing interest

The authors declare that they have no known competing financial interests or personal relationships that could have appeared to influence the work reported in this paper.

# References


1. A. Baeza, M. Manzano, M. Colilla, M. Vallet-Regi, Biomater. Sci. (2016) https://doi.org/10.1039/c6bm00039h.
2. Z.X. Li, J.C. Barnes, A. Bosoy, J.F. Stoddart, J.I. Zink, Chem. Soc. Rev. (2012) https://doi.org/10.1039/c1cs15246g

3. P. Yang, S. Gai, J. Lin, Chem. Soc. Rev. (2012) https://doi.org/10.1039/c2cs15308d
4. S.H. Yi, J.N. Zheng, P. Lv, D.J. Zhang, X.Y. Zheng, Y. Zhang, R.Q. Liao, Bioconjug. Chem. (2018) https://doi.org/10.1021/acs.bioconjchem.8b00416
5. R. Liu, X Zhao, T. Wu, P.Y. Feng, Am. Chem. Soc. (2008) https://doi.org/10.1021/ja8060886
6. Z. Luo, K.Y. Cai, Y. Hu, L. Zhao, P. Liu, L. Duan, W.H. Yang, Angew. Chem., Int. Ed. (2011) https://doi.org/10.1002/anie.201005061
7. C. Park, K. Oh, S. C. Lee and C. Kim, Angew. Chem., Int. Ed. (2007) https://doi.org/10.1002/anie.200603404
8. S. Angelos, Y.W. Yang, K. Patel, J.F. Stoddart and J.I. Zink, Angew. Chem., Int. Ed. (2008) https://doi.org/10.1002/anie.200705211
9. E. Aznar, L. Mondragón, J.V. Ros-Lis, F. Sancenón, M.D. Marcos, R. Martínez-Máñez, J. Soto, E. Pérez-Payá, P. Amorós, Angew. Chem., Int. Ed. (2011) https://doi.org/10.1002/anie.201102756
10. A. Schlossbauer, S. Warncke, P.M.E. Gramlich, J. Kecht D, A. Manetto, T. Carell, T. Bein, Angew. Chem., Int. Ed. (2010) https://doi.org/10.1002/anie.201000827
11. C. Coll, L. Mondragón, R. Martínez-Máñez, F. Sancenón, M.D. Marcos, J. Soto, P. Amorós E. Pérez-Payá, Angew. Chem., Int. Ed. (2011) https://doi.org/10.1002/anie.201004133
12. A. Bernardos, E. Aznar, M.D. Marcos, R. Martinez-Manez, F. Sancenon, J. Soto, J.M. Barat, P. Amoros, Angew. Chem., Int. Ed. (2009) https://doi.org/10.1002/anie.200900880
13. E. Che, Y.K. Gao, L. Wan, Y. Zhang, J.L. Bai, J. Li, Z. Sha, S.L. Wang, Micropor. Mesopor. Mat. (2015) https://doi.org/10.1016/j.micromeso.2014.11.013
14. T.T. Li, X. Shen, Y. Geng, Z.Y. Chen, L. Li, S. Li, H. Yang, C.H. Wu, H.J. Zeng, Y.Y. Liu, ACS. Appl. Mater. Inter. (2016) https://doi.org/10.1021/acsami.6b02963
15. N.K. Mal, M. Fujiwara, Y. Tanaka, Nature (2003) https://doi.org/10.1038/nature01362
16. Q.N. Lin, Q. Huang, C.Y. Li, C.Y. Bao, Z.Z. Liu, F.Y. Li, L.Y, Zhu, J. Am. Chem. Soc. (2010) https://doi.org/10.1021/ja103415t
17. Z.Y. Xiao, C.W. Ji, J.J. Shi, E.M. Pridgen, J. Frieder, J. Wu, O.C. Farokhzad, Angew. Chem., Int. Ed. (2012) https://doi.org/10.1002/ange.201204018
18. A. Natansohn, P. Rochon, Chem. Rev. (2002) https://doi.org/10.1021/cr970155y
19. E.W.G. Diau, J. Phys. Chem. A. (2004) https://doi.org/10.1021/jp031149a
20. J.W. Zhao, Z.S. He, B. Li, T.Y. Cheng, G.H. Liu, Mater. Sci. Eng. C. Mater. Biol. Appl. (2017) https://doi.org/10.1016/j.msec.2016.12.056
21. D.S. Wang, S. Wu, Langmuir (2016) https://doi.org/10.1021/acs.langmuir.5b04399
22. Y.Y. Wang, B. Li, L.M. Zhang, H. Song, L.G. Zhang, ACS Appl. Mater. Interfaces. (2013) https://doi.org/10.1021/am302492e
23. J.N. Liu, W.B. Bu. L.M. Pan. J.L. Shi, Angew. Chem., Int. Ed. (2013) https://doi.org/10.1002/ange.201300183

24. D. Tarn, D.P. Ferris, J.C. Barnes, M.W. Ambrogio, J.F. Stoddart, J.I. Zink, Nanoscale (2014) https://doi.org/10.1039/c3nr06049g.
25. G.F. Luo, W.H. Chen, H.Z. Jia, Y.X, Sun, H. Cheng, R.X. Zhuo, X.Z. Zhang. Nano. Res. (2015) https://doi.org/10.1007/s12274-014-0698-2
26. N.G. Liu, D.R. Dunphy, M.A. Rodriguez, S. Singer, J. Brinker, Chem. Comm. (2003) https://doi.org/10.1039/b301569f
27. C.Yu, H. Chu, Y. Wan, D. Zhao, J. Mater. Chem. (2010) https://doi.org/10.1039/b925864g
28. Z.P. Xu, P.S. Braterman, J. Mater. Chem. (2003) https://doi.org/10.1039/b207540g
29. R. Harrison, L. Li, Z. Gu, Z.P. Xu, Micropor. Mesopor. Mat. (2017) https://doi.org/10.1016/j.micromeso.2016.04.031
30. W.T, Wang, T. Huang, W.C. Law, C.H. Cheng, C.Y. Tang, L. Chen, X.H. Gong, Z.F. Liu, S.J. Long, J. Phys. Chem. C. (2018) https://doi.org/10.1021/acs.jpcc.7b11026
31. Q.L. Li, L.G. Wang, X.L. Qiu, Y.L. Sun, P.X. Wang, Y. Liu, F. Li, A.D. Qi, H. Gao, Y.W. Yang, Poly. Chem. (2014) https://doi.org/10.1039/c4py00041b
32. L. Sharma, T. Matsuoka, T. Kimura, H. Matsuda, Polym. Adv. Technol. (2002) https://doi.org/10.1002/pat.214
33. R. Schmidt, E. Mcnellis, W. Freyer, D. Brete, T. Giessel, C. Gahl, Appl. Phys. A. (2008) https://doi.org/10.1007/s00339-008-4829-z
34. D.S. Wang, D.Y. Xie, W.B. Shi, S.D. Sun, C.S. Zhao, Langmuir (2013) https://doi.org/10.1021/la401201w
35. M.J. Barnabas, S. Parambadath, C.S. Ha, J. Ind. Eng. Chem. (2017) https://doi.org/10.1016/j.jiec.2017.05.011
36. D.P. Ferris, Y.L. Zhao, N.M. Khashab, H.A. Khatib, J.F. Stoddart, J.I. Zink, J. Am. Chem. Soc. (2009) https://doi.org/10.1021/ja807798g
37. C.B. Gong, Y.Z. Yang, Y.H. Yang, A.X. Zheng, S. Liu, Q. Tang, J. Colloid. Interface. Sci. (2016) https://doi.org/10.1016/j.jcis.2016.07.039

# Figures

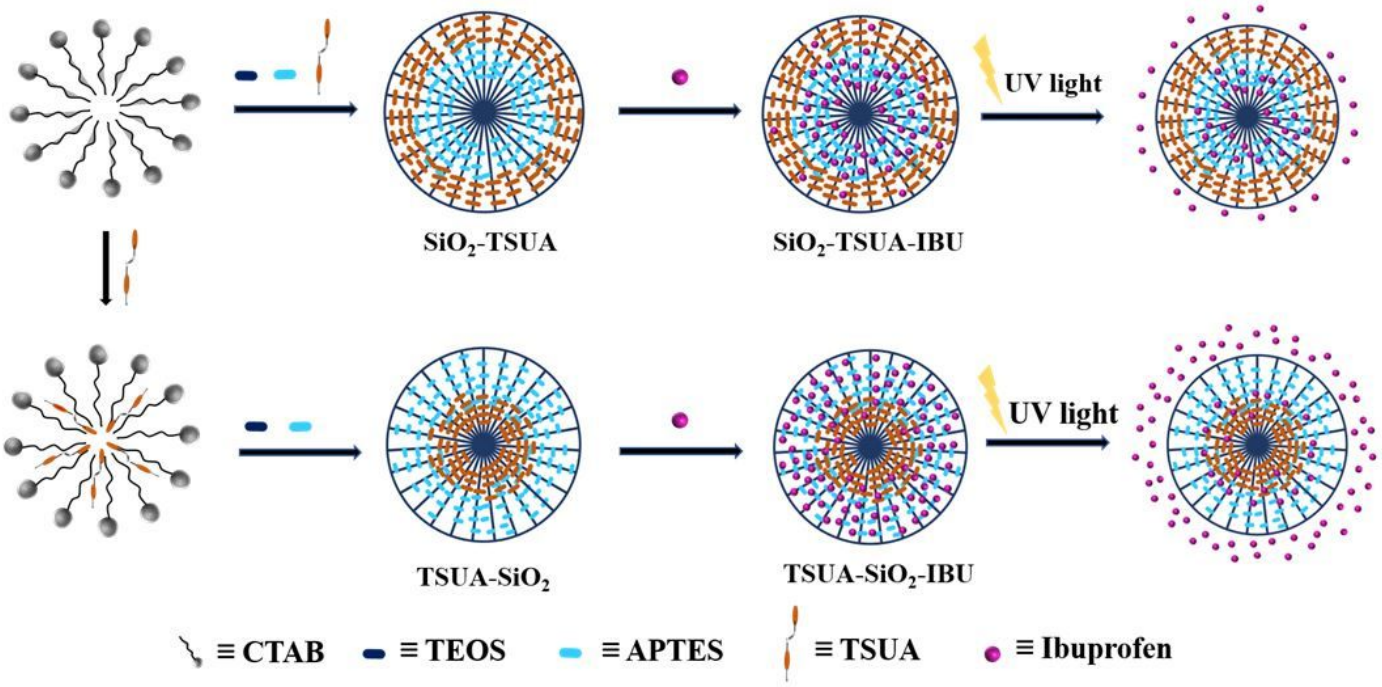


## Figure 1

Scheme representation of the structure, group dispersion and the photo response ability of the target nanoparticles.

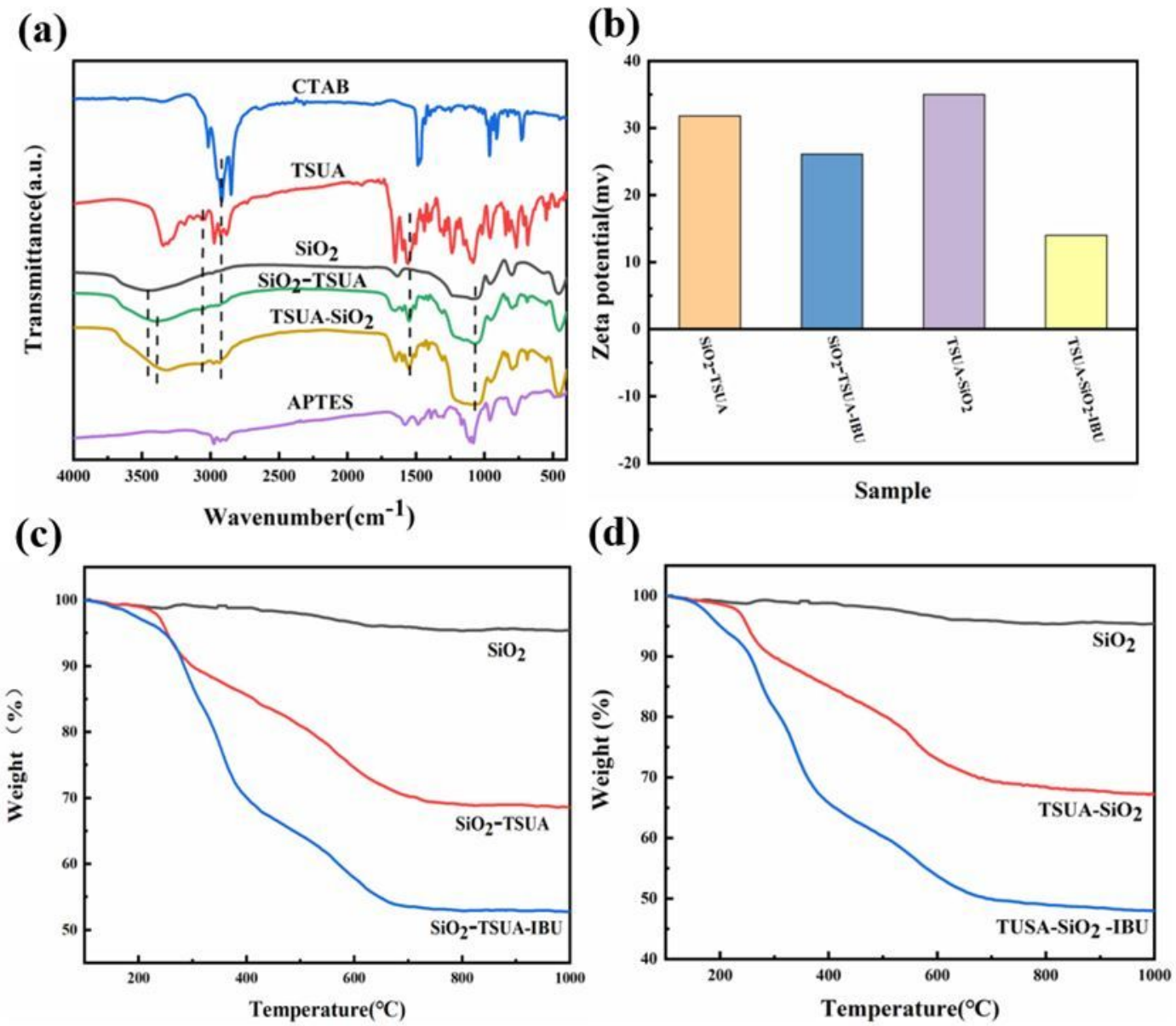


## Figure 2

(a)FTIR spectra of CTAB, TSUA, $SiO_2$, APTES, $SiO_2$-TSUA and TSUA-$SiO_2$. (b)Zeta potential of $SiO_2$-TSUA and TSUA-$SiO_2$. (c,d)TGA curves of $SiO_2$-TSUA and TSUA-$SiO_2$ as well as the IBU loaded corresponding samples.

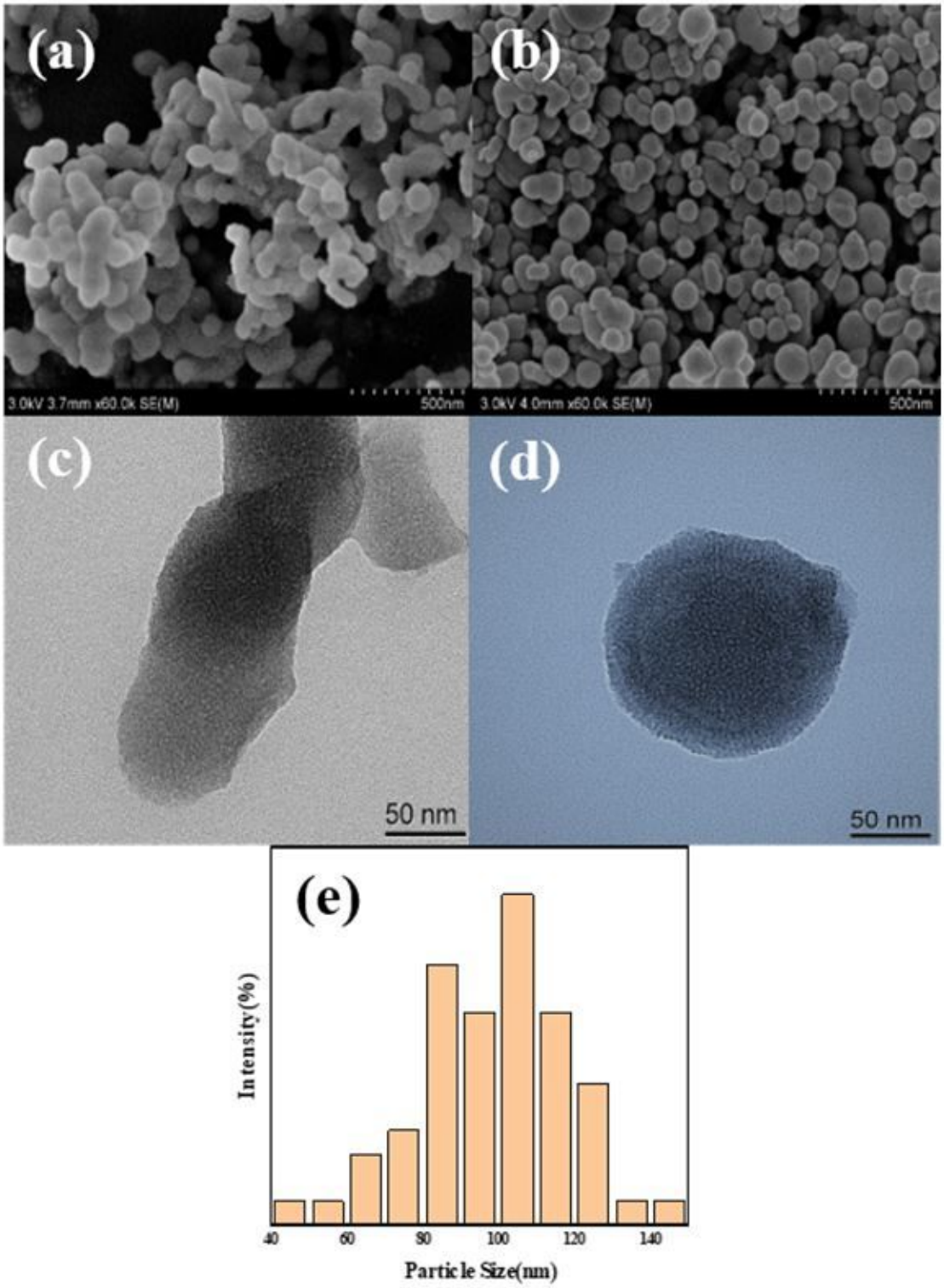


## Figure 3

SEM (a, b) and TEM (c, d) images of $SiO_2$-TSUA (a, c) and TSUA-$SiO_2$ (b, d) as well as the particle size distribution of TSUA-$SiO_2$ (e).

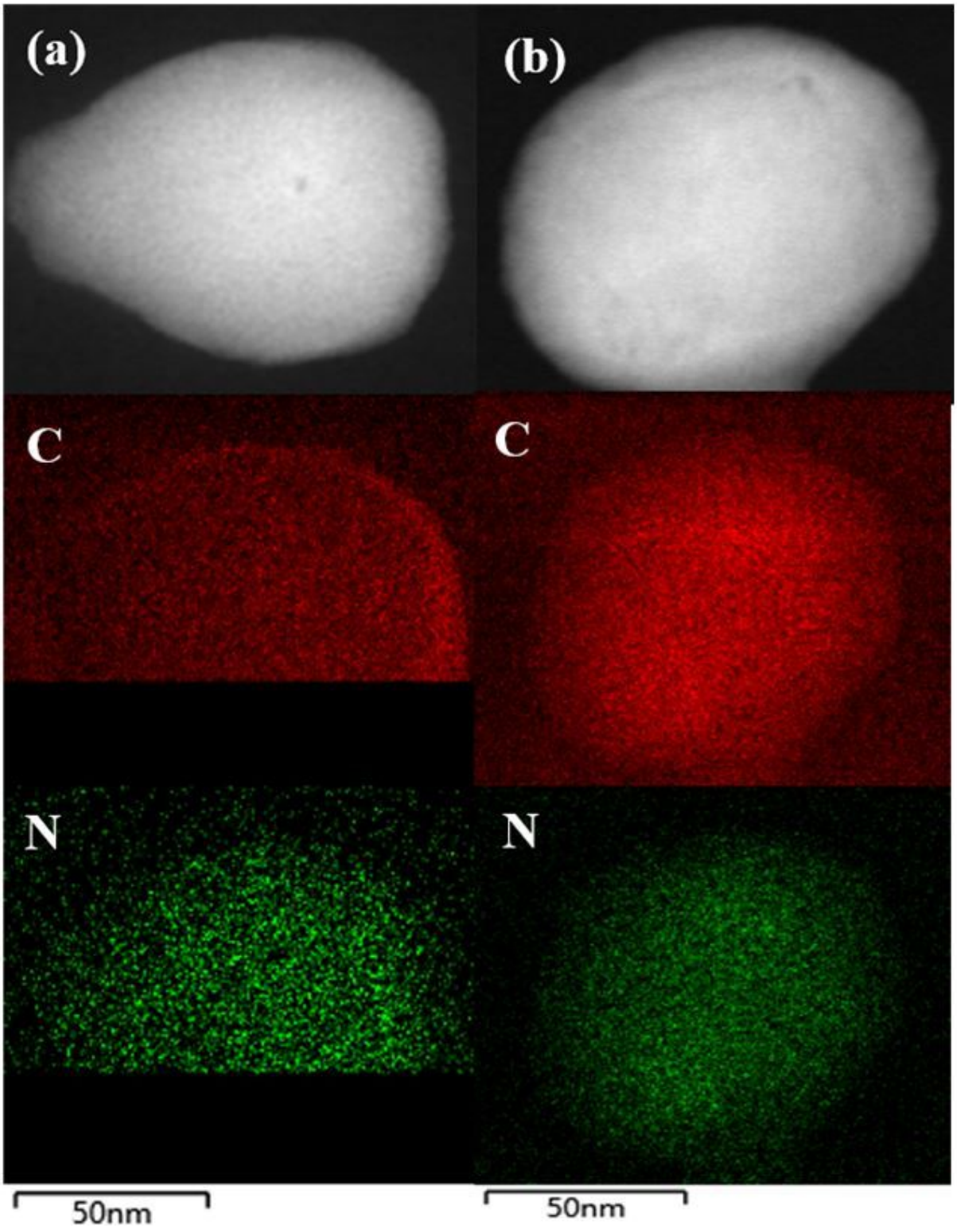


## Figure 4

Elements dispersion of $SiO_2$-TSUA (a) and TSUA-$SiO_2$ (b).

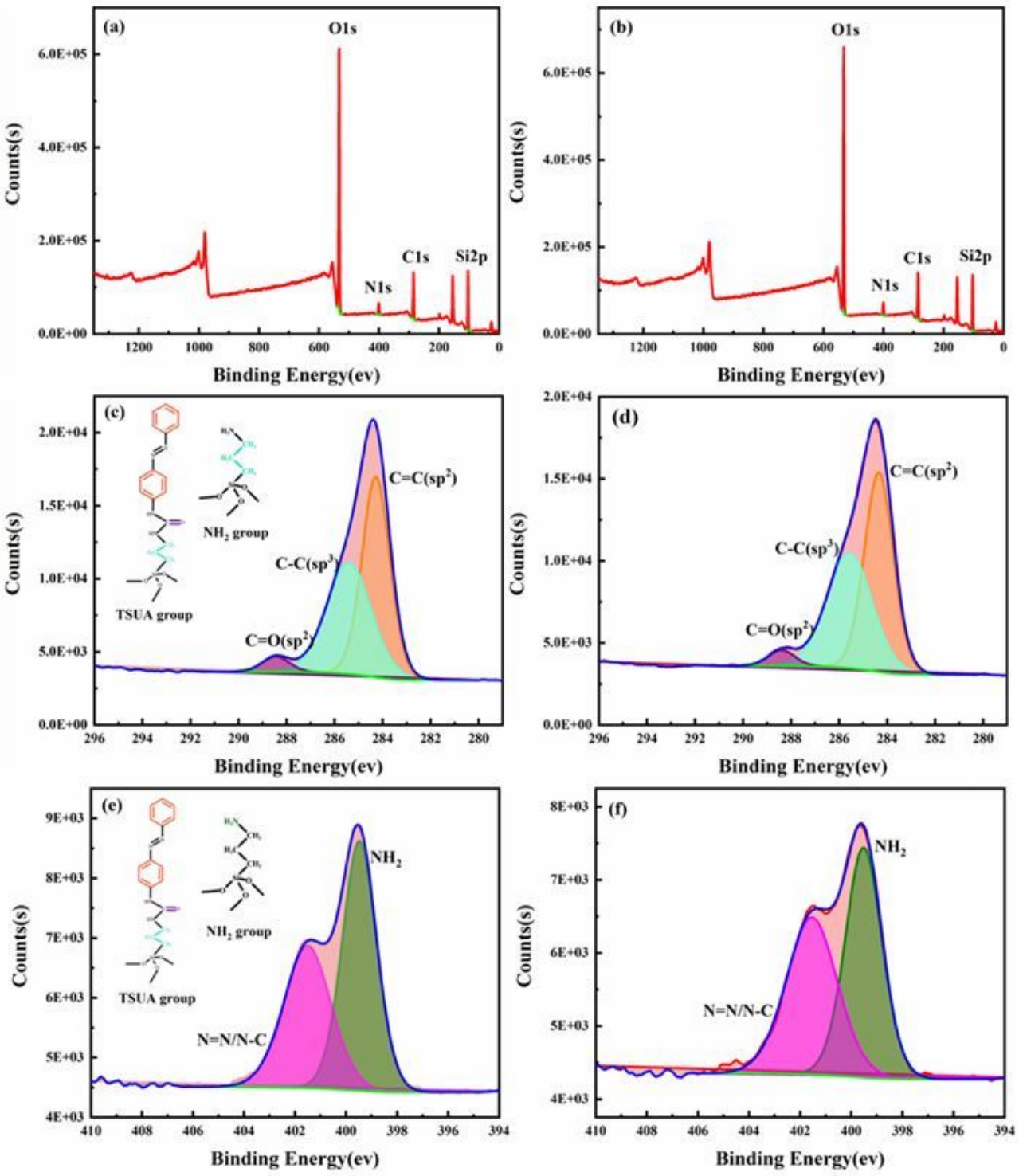


## Figure 5

XPS of spectra of $SiO_2$-TSUA (a) and TSUA-$SiO_2$ (b) and their corresponding binding energy of C1s region (c, d) and N1s region (e, f).

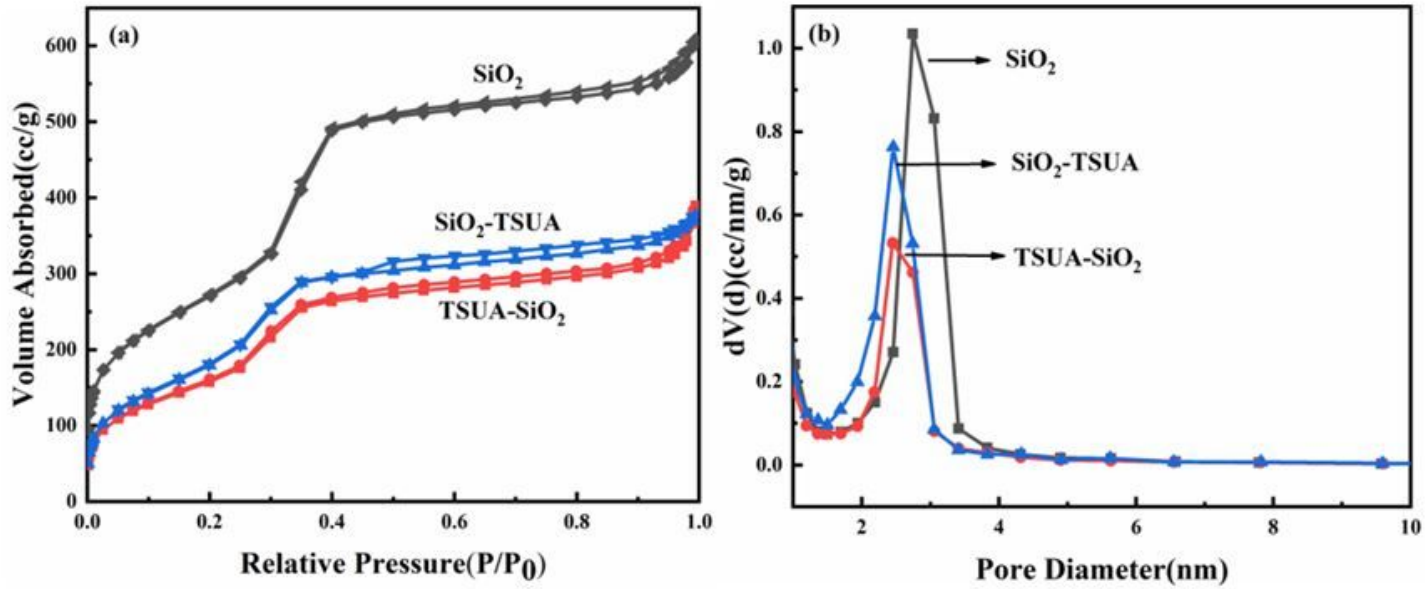


## Figure 6

Nitrogen adsorption-desorption isotherms (a) and pore size distributions (b) of $SiO_2$, $SiO_2$-TSUA and TSUA-$SiO_2$.

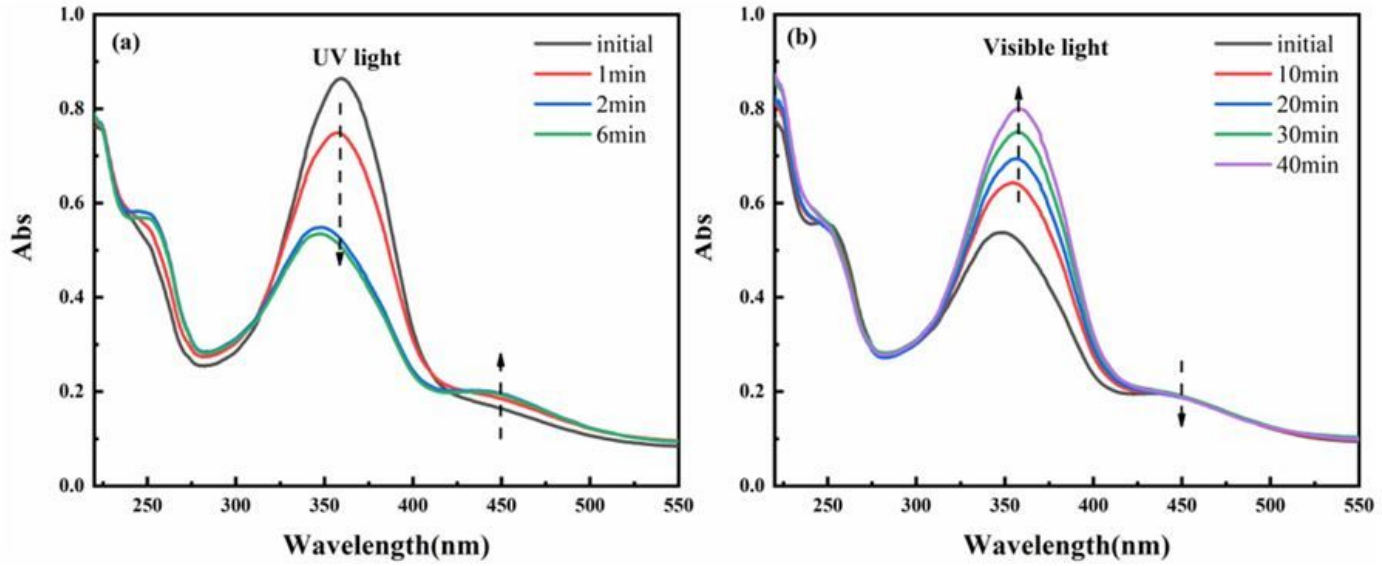


## Figure 7

UV–Vis absorption spectral changes of TSUA-$SiO_2$ in response to the (a) UV and (b) visible light.

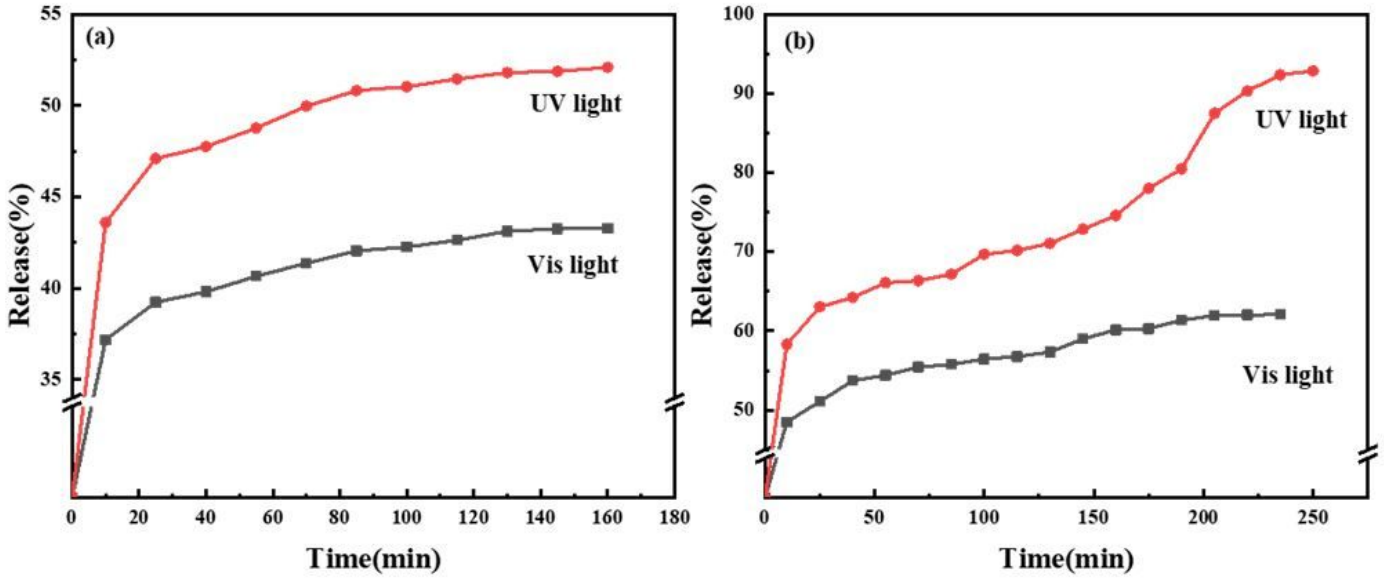


## Figure 8

Release percent of IBU by $SiO_2$-TSUA (a) and TSUA-$SiO_2$ (b) irradiated by visible and UV light.

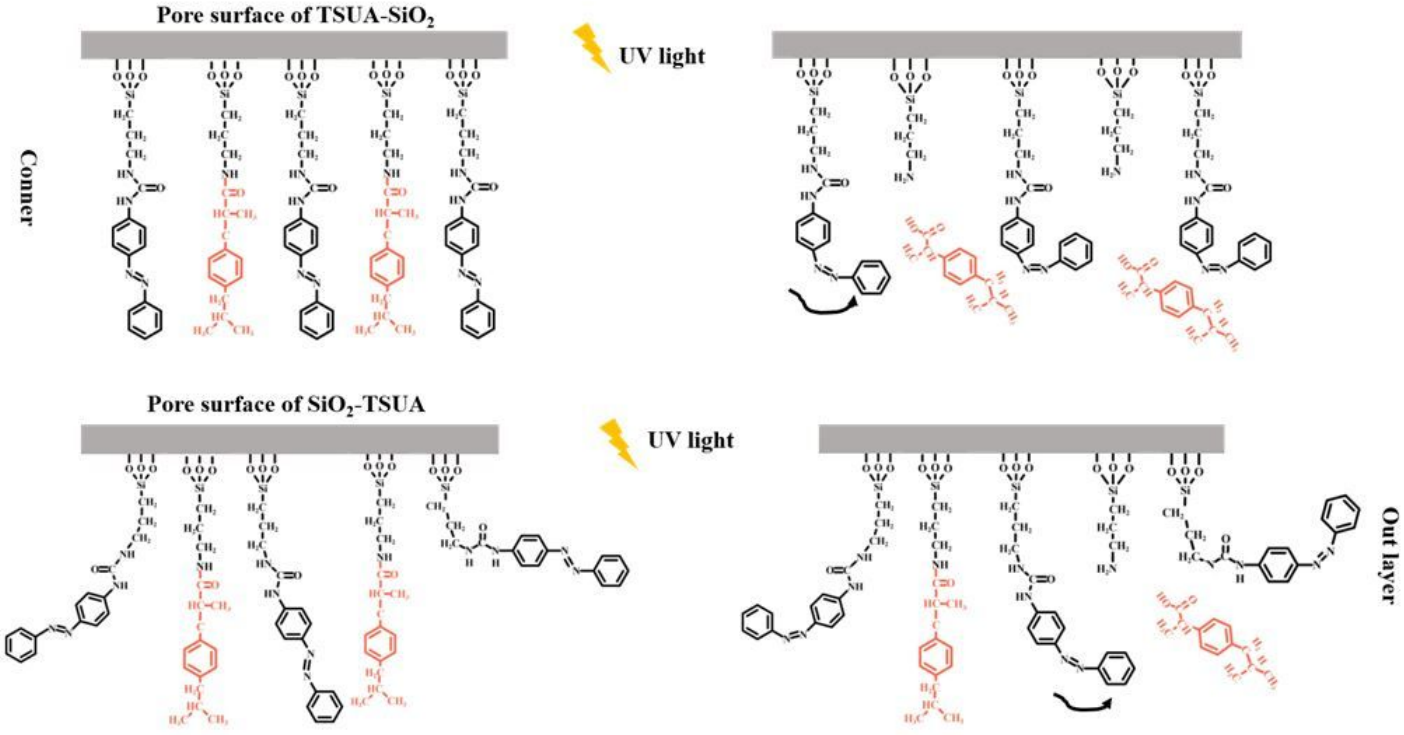


## Figure 9

Conformation and interaction changes between azobenzene, -$NH_2$ and the drugs.